Journal of Sound and Vibration (2002) **249**(3), 611–621
doi:10.1006/jsvi.2001.3742, available online at http://www.idealibrary.com on IDEAL®

ROBUSTNESS ANALYSIS OF AN ENVIRONMENTAL ACTIVE NOISE CONTROL SYSTEM

J. YANG, S.-E. TAN AND W.-S. GAN

Digital Signal Processing Lab, School of Electrical & Electronic Engineering, Nanyang Technological University, Singapore 639798, *Singapore. E-mail: ewsgan@ntu.edu. sg*

(*Received* 28 *September* 2000, *and in final form* 30 *May* 2001)

1. INTRODUCTION

Most of the work on active noise control is confined to free field and restricted spaces such as ducts and enclosures [1, 2]. Recently, control of sound in an unconfined space has drawn increased attention [3–7]. More recently, there has been a concentrated effort to develop practical control systems for environmental noise reduction [8]. In reference [8], the stability condition was given of the electronically controlled acoustic shadow (ECAS) system, and a two-channel system is used initially to demonstrate the basic properties. However, the basic properties of the two-channel plant do not seem to exist in the multichannel plant, as shown in the matrix condition spectra; the six-channel ECAS system has different number of peaks from the three-channel system, although they were expected to have the same positions of peaks according to the derived formula in reference [8]. This gave considerable motivation to our present study on the robustness of multichannel ECAS system.

It is found that the positions of peaks occur when the largest path difference between the sources and detectors corresponds to multiples of one wavelength for the case of three-four- and six- channel systems. This is confirmed by numerical simulation and is helpful to determine the robustness of control system.

2. ACOUSTIC ROBUSTNESS OF TWO-CHANNEL SYSTEM

The freefield ECAS system is illustrated in Figure 1. It is a symmetric configuration of primary sources, secondary sources and sensors. For simplicity, the primary sources are not shown in the figure. The sound field radiated from a monopole source can be written as

$$p = \mathrm{j}\omega\rho_0 q \frac{\exp(-\mathrm{j}kr)}{4\pi r}, \tag{1}$$

where ω is the angular frequency, ρ_0 is the density of the medium, q is the source strength, k is the wave number $2\pi/\lambda$, λ being the wavelength, and r is the distance from the source to the field point. If Q is defined as strength term $Q = \mathrm{j}\omega\rho_0 q/4\pi$, which is the time derivative of the source strength, then the transfer function C_{mn} between the nth monopole source (secondary source) and the mth target point (microphone) is given by $C_{mn} = \mathrm{e}^{-\mathrm{j}kr_{mn}}/r_{mn}$. In

0022-460X/02/030611 + 11 $35.00/0

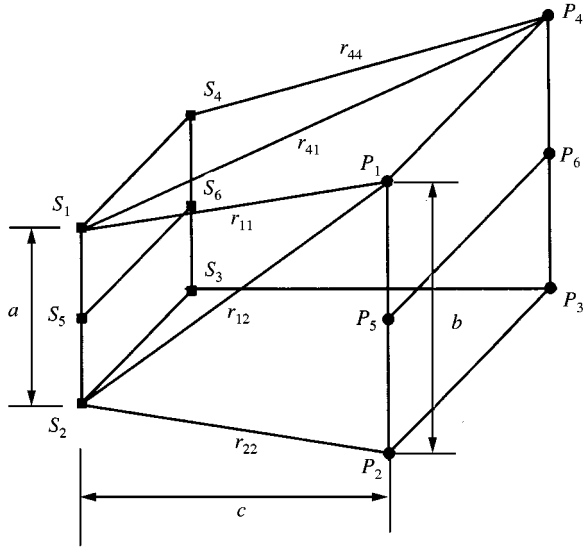

Figure 1. ECAS geometry: ■, secondary sources; ●, sensors.

the performance analysis of ECAS system, the condition number is used as the robustness measurement, given by [8]

$$K = \varepsilon_{max}/\varepsilon_{min}, \tag{2}$$

where ε_{max} and ε_{min} are the largest and smallest eigenvalues of the transfer function matrix $C^H C$ respectively.

For the two-channel system which consists of sound sources 1 and 2 and sensors 1 and 2, $r_{11} = r_{22}$, $r_{12} = r_{21}$, we can get the transfer function matrix

$$C = \begin{bmatrix} C_{11} & C_{12} \\ C_{12} & C_{11} \end{bmatrix} = \begin{bmatrix} e^{-jkr_{11}}/r_{11} & e^{-jkr_{12}}/r_{12} \\ e^{-jkr_{12}}/r_{12} & e^{-jkr_{11}}/r_{11} \end{bmatrix} \tag{3}$$

and then

$$C^{\mathrm{H}}C = \begin{bmatrix} |C_{11}|^2 + |C_{12}|^2 & C_{11}^* C_{12} + C_{11} C_{12}^* \\ C_{11}^* C_{12} + C_{11} C_{12}^* & |C_{11}|^2 + |C_{12}|^2 \end{bmatrix} \triangleq \begin{bmatrix} C_1 & C_2 \\ C_2 & C_1 \end{bmatrix}, \tag{4}$$

where both C_1 and C_2 are real, and the superscript H is the Hermitian transpose of a vector. The eigenvalues of $C^{\mathrm{H}}C$ are the roots of the characteristic equation $\det[C^{\mathrm{H}}C - \varepsilon I] = 0$, and I is the identity matrix of rank 2. Clearly, the eigenvalues ε are, respectively, the sum and difference between the diagonal and corner values of the matrix $C^{\mathrm{H}}C$, given by

$$\varepsilon_{1,2} = C_1 \pm C_2 = |C_{11}|^2 + |C_{12}|^2 \pm 2|C_{11}C_{12}|\cos\phi, \tag{5, 6}$$

where $\phi = k\delta r$ is the phase difference, which plays a role in determining the extreme value of condition number. $\delta r = r_{12} - r_{11}$ denotes the path difference between each source and the microphone. It approximates to $ab/2c$, providing $c \gg (b + a)$, where a, b and c have meanings illustrated in Figure 1.

From equations (5) and (6), condition number defined in equation (2) takes on a minimum value, $K_{min} = 1$, when

$$\cos\phi = 0 \qquad \text{i.e., } \delta r = (2p-1)\lambda/4, \quad \text{where } p = 1,2,3,\ldots. \tag{7}$$

The transfer function matrix is said to be well-conditioned, resulting in the most robust control system [9]. The positions of the valleys in the condition number can be obtained as

$$f_p = c_0/\lambda = (p-1/2)c_0(c/ab), \quad \text{where } p = 1,2,3,\ldots. \tag{8}$$

It shows that for good cancellation performance, the adaptive system should be operated close to the valley frequencies, and a wide valley is needed. On the other hand, the condition number takes the maximum, $K_{max} = [(r_{12}/r_{11}+1)/(r_{12}/r_{11}-1)]^2$, when

$$|\cos\phi| = 1 \qquad \text{i.e., } \delta r = q\lambda/2, \quad \text{where } q = 0,1,2,3,\ldots. \tag{9}$$

The transfer function matrix is said to be ill-conditioned, resulting in the least robust control system [9]. Similarly, the positions of the peaks in the condition number can be found as

$$f_q = c_0/\lambda = qc_0(c/ab), \quad \text{where } q = 0,1,2,3,\ldots, \tag{10}$$

which is the same as equation (75) in reference [8]. These peaks must be avoided to assure system convergence.

From the point of view of the practical application, except to widen the stability region of adaptive system, it draws more attention to determine the condition peaks in frequency domain. Consider equations (5) and (6); the eigenvalues are bounded, the positions of condition peaks depend more on the smaller eigenvalue rather than the larger one. This property will be used in the following robustness analysis of multichannel system.

3. MULTICHANNEL CONDITION SPECTRA

In the case of three-channel system, i.e., sensors 1, 5 and 2 correspond to the sound sources 1, 5 and 2 respectively (see Figure 1). The transfer function (3×3 matrix) can be written as

$$C^{\mathrm{H}}C = \begin{bmatrix} C_1 & C_2 & C_3 \\ C_2^* & C_4 & C_2^* \\ C_3 & C_2 & C_1 \end{bmatrix}, \tag{11}$$

where C_1, C_3 and C_4 are real, and C_2 is complex, and their explicit expressions are given in (A1)–(A4) in Appendix A. The eigenvalues can be obtained as

$$\varepsilon_1 = C_1 - C_3 = |C_{11}|^2 + |C_{12}|^2 - 2|C_{11}C_{12}|\cos\phi, \tag{12}$$

$$\varepsilon_2 = \tfrac{1}{2}(C_1 + C_3 + C_4 - \sqrt{\Delta}), \qquad \varepsilon_3 = \tfrac{1}{2}(C_1 + C_3 + C_4 + \sqrt{\Delta}), \tag{13, 14}$$

where $\Delta = (C_1 + C_3 - C_4)^2 + 8|C_2|^2$. It can be easily seen from equations (12)–(14) that $\varepsilon_{1,2,3} > 0$ and $\varepsilon_2 < \varepsilon_3$. From equations (13) and (A5) in Appendix A, the eigenvalue ε_2 has its minimum when $|C_2|$ is maximized, i.e., $\cos(\phi/2) = 1$. However, from equation (12), the eigenvalue ε_1 is minimum when $\cos\phi = 1$. Therefore, half the number of condition peaks

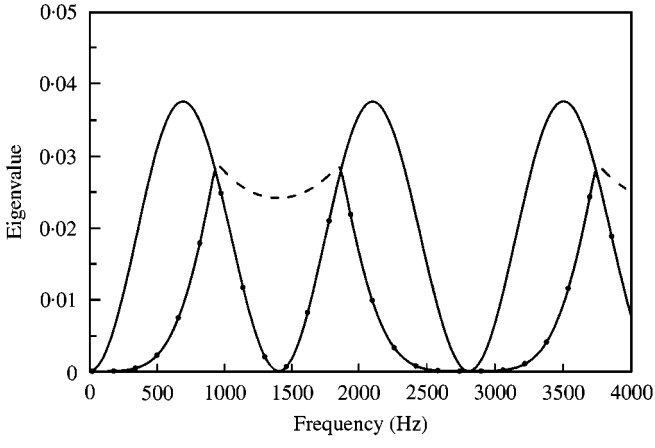

Figure 2. Eigenvalue spectra of the three-channel system. —·—, ε_{min}; ——, ε_1; – – –, ε_2.

will be lost by analyzing the eigenvalue ε_2. This is verified by the numerical computation as shown in Figure 2. Now the positions of peaks frequencies can be found from the equation

$$\cos\phi = 1 \qquad \text{i.e., } \delta r = q\lambda, \quad \text{where } q = 0, 1, 2, 3, \ldots \tag{15}$$

and one gets

$$f = c_0/\lambda = qc_0(2c/ab), \quad \text{where } q = 0, 1, 2, 3, \ldots. \tag{16}$$

It shows that maxima in the condition spectra occur when the largest path difference between the sources and detectors corresponds to the multiples of wavelengths. This is different from the case of two-channel system.

In the case of four-channel system, i.e., sensors 1, 2, 3 and 4 correspond to the sound sources 1, 2, 3 and 4, respectively (see Figure 1). The transfer function (4×4 matrix) can be written as

$$C^{\mathrm{H}}C = \begin{bmatrix} C_1 & C_2 & C_3 & C_2 \\ C_2 & C_1 & C_2 & C_3 \\ C_3 & C_2 & C_1 & C_2 \\ C_2 & C_3 & C_2 & C_1 \end{bmatrix}, \tag{17}$$

where C_1, C_2 and C_3 are all real, and their explicit expressions are given in (A6)–(A8) in Appendix A. Equation (17) is the circular or periodic Toeplitz matrix, and its eigenvalues can be expressed in terms of exact algebraic (periodic) functions [10] as

$$\varepsilon_n = C_1 + 2C_2\cos(n\pi/2) + C_3\cos(n\pi), \quad n = 1, 2, 3, 4, \tag{18}$$

i.e., $\varepsilon_1 = C_1 - C_3$, $\varepsilon_2 = C_1 - 2C_2 + C_3$, $\varepsilon_3 = \varepsilon_1$ and $\varepsilon_4 = C_1 + 2C_2 + C_3$. Substituting equations (A6)–(A9) into equation (18), we have

$$\varepsilon_1 = \varepsilon_3 = |C_{11}|^2 + |C_{13}|^2 - 2|C_{11}C_{13}|\cos\phi', \tag{19}$$

$$\varepsilon_2 = |C_{11}|^2 + 4|C_{12}|^2 + |C_{13}|^2 - 4(|C_{11}C_{12}| + |C_{12}C_{13}|)\cos\phi + 2|C_{11}C_{13}|\cos\phi', \tag{20}$$

$$\varepsilon_4 = |C_{11}|^2 + 4|C_{12}|^2 + |C_{13}|^2 + 4(|C_{11}C_{12}| + |C_{12}C_{13}|)\cos\phi + 2|C_{11}C_{13}|\cos\phi', \tag{21}$$

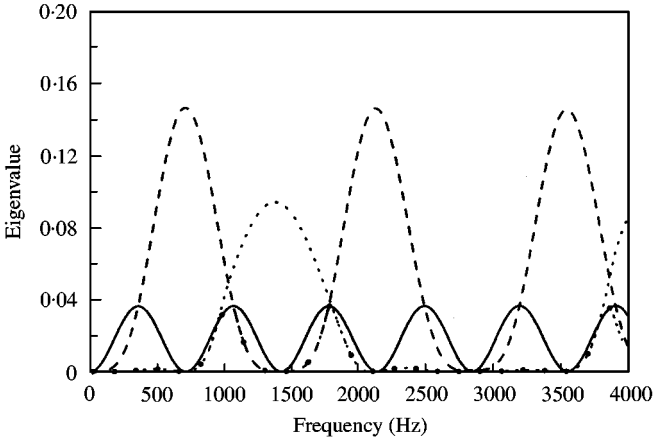

Figure 3. Eigenvalue spectra of the four-channel system. —·—, ε_{min}; – – –, ε_1; · · · · ·, ε_2; ——, ε_4.

where the term $\cos\phi'$ is contained in all eigenvalues. It is interesting to note that when $\cos\phi' = 1$, eigenvalue $\varepsilon_1(\varepsilon_3 = \varepsilon_1)$ is at its minimum, and at the same time one of the eigenvalues ε_2 or ε_4 has its minimum due to $\cos\phi = 1$ or -1, and their extreme values occur alternatively in the frequency domain. This can be seen in Figure 3. Like the three-channel system, it will lose half the number of condition peaks if only the eigenvalue ε_2 or ε_4 is analyzed. So the positions of the peaks can be found from the equation

$$\cos\phi' = 1, \qquad \text{i.e., } \delta r' = q\lambda, \quad \text{where } q = 0, 1, 2, 3, \ldots. \tag{22}$$

Combining $\delta r' \approx ab/c$, one gets

$$f = qc_0(c/ab), \quad \text{where } q = 0, 1, 2, \ldots, n, \tag{23}$$

which is the same as equation (10) for the two-channel system. However, maxima in the condition spectra occur when the largest path difference between the sources and detectors (i.e., $r_{13} - r_{11}$) corresponds to the multiples of wavelengths.

In the case of six-channel system, sensors 1, 5, 2, 3, 6 and 4 correspond to the sound sources 1, 5, 2, 3, 6 and 4 respectively (see Figure 1). The transfer function (6×6 matrix) can be written in the partitioned matrix form

$$C^{\mathrm{H}}C = \left[\begin{array}{ccc|ccc} C_1 & C_2 & C_3 & C_4 & C_5 & C_6 \\ C_2^* & C_7 & C_2^* & C_5^* & C_8 & C_5^* \\ C_3 & C_2 & C_1 & C_6 & C_5 & C_4 \\ \hline C_4 & C_5 & C_6 & C_1 & C_2 & C_3 \\ C_5^* & C_8 & C_5^* & C_2^* & C_7 & C_2^* \\ C_6 & C_5 & C_4 & C_3 & C_2 & C_1 \end{array}\right] = \begin{bmatrix} A_1 & A_2 \\ A_2 & A_1 \end{bmatrix}, \tag{24}$$

where

$$A_1 = \begin{bmatrix} C_1 & C_2 & C_3 \\ C_2^* & C_7 & C_2^* \\ C_3 & C_2 & C_1 \end{bmatrix} \quad \text{and} \quad A_2 = \begin{bmatrix} C_4 & C_5 & C_6 \\ C_5^* & C_8 & C_5^* \\ C_6 & C_5 & C_4 \end{bmatrix}. \tag{25, 26}$$

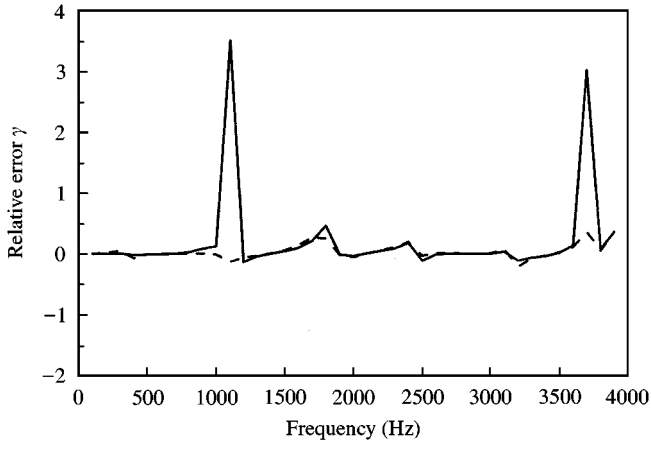

Figure 4. The relative error $\gamma = (\alpha_2 - \alpha_2^*)/\alpha_2$ versus frequency. ——, γ_{real}; – – –, γ_{imag}.

All the elements except C_2 and C_5 in matrix $C^{\text{H}}C$ are real. Their explicit expressions are given in equations (A10)–(A17) in Appendix A. When the submatrices A_1 are non-singular, the determinant of $C^{\text{H}}C$ is given by [10]

$$\det(C^{\text{H}}C) = \det(A_1) \times \det(A_1 - A_2 A_1^{-1} A_2). \tag{27}$$

In the case of eigenvalues, generally no exact formula can exist for a 5×5 or higher rank matrix [11], except for the special ones. Fortunately, $A_1 A_2 = A_2 A_1$ basically holds except at a few frequencies as shown in Figure 4, due to geometry $c \gg (b + a)$. The expressions of $A_1 A_2$ and $A_2 A_1$ and definition of γ are given in Appendix A. Therefore, equation (27) yields

$$\det(C^{\text{H}}C) = \det(A_1^2 - A_2^2) = \det(A_1 + A_2) \times \det(A_1 - A_2). \tag{28}$$

The eigenvalue solution (12)–(14) in the three-channel system can be used here. For the matrix $A_1 + A_2$, we have eigenvalues

$$\varepsilon_1 = |C_{11}|^2 + 4|C_{12}|^2 + |C_{13}|^2 - 4(|C_{11}C_{12}| + |C_{12}C_{13}|)\cos\phi + 2|C_{11}C_{13}|\cos\phi', \tag{29}$$

$$\varepsilon_2 = \tfrac{1}{2}[(C_1 + C_3 + C_7) + (C_4 + C_5 + C_8) - \sqrt{\Delta_1}], \tag{30}$$

$$\varepsilon_3 = \tfrac{1}{2}[(C_1 + C_3 + C_7) + (C_4 + C_5 + C_8) + \sqrt{\Delta_1}], \tag{31}$$

where $\phi' = k\delta r' = 2\phi$, $\Delta_1 = [(C_1 + C_3 - C_7) + (C_4 + C_5 - C_8)]^2 + 8|C_2 + C_5|^2$. For the matrix $A_1 - A_2$, we have eigenvalues

$$\varepsilon_4 = |C_{11}|^2 + |C_{13}|^2 - 2|C_{11}C_{13}|\cos\phi', \tag{32}$$

$$\varepsilon_5 = \tfrac{1}{2}[(C_1 + C_3 + C_7) - (C_4 + C_5 + C_8) - \sqrt{\Delta_2}], \tag{33}$$

$$\varepsilon_6 = \tfrac{1}{2}[(C_1 + C_3 + C_7) - (C_4 + C_5 + C_8) + \sqrt{\Delta_2}], \tag{34}$$

where $\Delta_2 = [(C_1 + C_3 - C_7) - (C_4 + C_5 - C_8)]^2 + 8|C_2 - C_5|^2$. Equations (29) and (30) imply that $\varepsilon_2 < \varepsilon_3$ and similarly $\varepsilon_5 < \varepsilon_6$ from equations (32) and (33), so only the eigenvalues analysis of ε_1, ε_2, ε_4 and ε_5 is needed for obtaining the condition peaks positions. Like the eigenvalue analysis in the three- and four-channel systems, we will lose half the number of

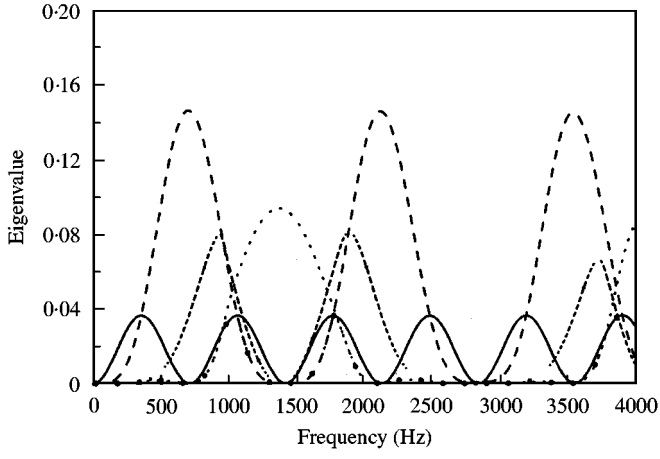

Figure 5. Eigenvalue spectra of the six-channel system. —·—, ε_{min}; – – –, ε_1; · · · ·, ε_2; ——, ε_4; —·—·—·—, ε_5.

condition peaks if we only consider one of the eigenvalues ε_1, ε_2 and ε_5 as shown in Figure 5. Thus, eigenvalue ε_4 is chosen, and is at its minimum when $\cos\phi' = 1$. The peaks of condition number occur at the frequencies

$$f = qc_0(c/ab), \quad \text{where } q = 0, 1, 2, \ldots, n. \tag{35}$$

which is the same as the formulations for two- and four-channel systems. Again, maxima in the condition spectra occur when the largest path difference between the sources and detectors (i.e., $r_{13} - r_{11}$) corresponds to the multiples of wavelengths.

4. SIMULATIONS AND DISCUSSION

In this paper, a similar model as that in reference [8] is adopted. For the ECAS system shown in Figure 1, the parameters are $a = 1\,\text{m}$, $b = 1\,\text{m}$, $c = 10\,\text{m}$, and speed of sound $c_0 = 343\,\text{m/s}$. Figures 2, 3 and 5 show the multichannel eigenvalues (related to the condition number) versus frequency for the three-channel (1 layer of 3), four-channel (2 layers of 2) and six-channel (2 layers of 3) systems respectively. ε_{min} represents the smallest one in the eigenvalues of the multichannel transfer function matrix. Apart from the special case of two-channel system, the positions of condition peaks can be obtained by analyzing the eigenvalue in the form

$$\varepsilon = |C_{11}|^2 + |C_{1n}|^2 - 2|C_{11}C_{1n}|\cos(kr_{11} - kr_{1n}), \tag{36}$$

where $n = 2, 3, 3$ corresponds to the three- and four- and six-channel systems respectively. This means that maxima in the condition spectra occur when the largest path difference between the sources and sensors corresponds to the multiples of wavelengths.

To verify the effectiveness of the method described in the eigenvalue analysis of six-channel system, all the eigenvalues from equations (29)–(34) are drawn in Figure 6, and the numerical eigenvalue solutions to equation (24) by the use of MATLAB are also depicted in that figure. It can be seen that all the numerical eigenvalues collapse on the eigenvalue spectra, so the relative error γ given in Figure 4 does not affect the eigenvalue solutions to equation (24) when using the exact formulas (29)–(34).

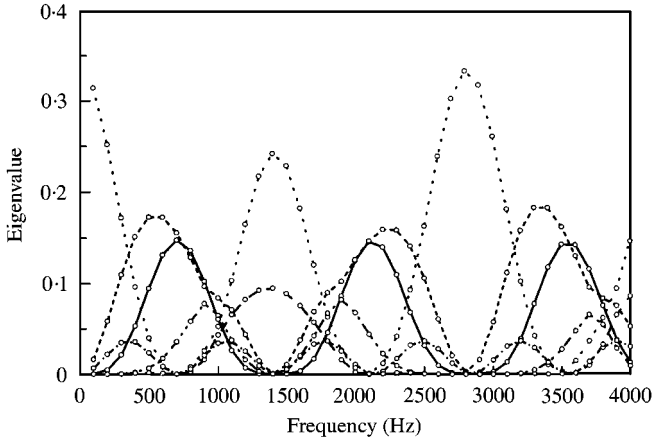

Figure 6. Comparison of eigenvalues of the six-channel system from equations (29)–(34) and equation (24) respectively. ——, ε_1; – – –, ε_2; · · · ·, ε_3; —·—·—, ε_4; —·-—·-—; ε_5; ----, ε_6; 0, numerical eigenvalues.

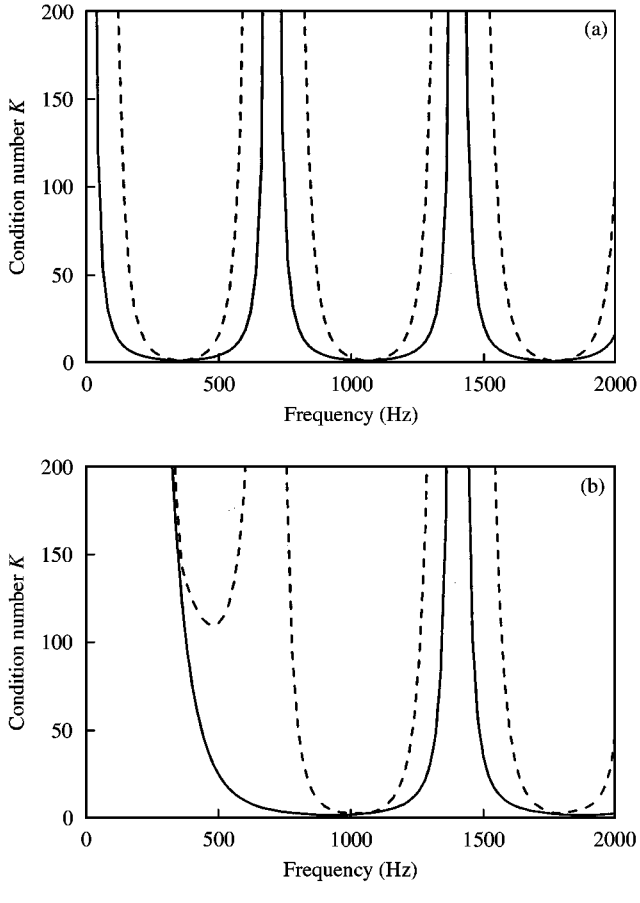

Figure 7(a). Multichannel system condition spectra. (a) ———, two channels; ———, four channels. (b) ———, three channels; ———, six channels.

Finally, the multichannel condition spectra for two- and four- and three- and six-channel systems are summarized in Figure 7(a) and 7(b). It indicates that: first, the eigenvalue expressed in equation (36) is only applicable to determine the condition peaks positions; second, other eigenvalues shown in Figures 2, 3 and 5 are responsible for the peaks width. It also indicates that the peaks thicken as the channel number increases as mentioned in reference [8].

5. CONCLUSION

This paper has given a detailed eigenvalue analysis for establishing robust control system. It facilitates the determination of condition peaks. For moderate channel numbers, the condition peaks occur when the largest path difference between the sources and sensors corresponds to multiples of one wavelength. The simulation results are helpful to understand the acoustic robustness and to predict the stability region in frequency domain. The robustness analysis in this paper has potential application prospect for achieving effective noise control.

REFERENCES

1. P. A. NELSON and S. J. ELLIOTT 1992 *Active Control of Sound*. London: Academic Press.
2. P. A. HANSEN and S. D. SYNDER 1997 *Active Control of Noise and Vibration*. London: E&FN Spon.
3. A. OMOTO and K. FUJIWARA 1993 *Journal of the Acoustical Society of America* **94**, 2173–2180. A study of an actively controlled noise barrier.
4. P. JOSEPH, S. J. ELLOITT and P. A. NELSON 1994 *Journal of Sound and Vibration* **172**, 605–627. Near field zones of quiet.
5. S. E. WRIGHT and B. VUKSANOVIC 1996 *Journal of Sound and Vibration* **190**, 565–585. Active control of environmental noise.
6. J. GUO, J. PAN and C. BAO 1997 *Journal of the Acoustical Society of America* **101**, 1492–1501. Actively created quiet zones by multiple control sources in free space.
7. X. QIU, C. H. HANSEN and X. LI 1998 *Journal of Sound and Vibration* **215**, 81–103. A comparison of near-field acoustic error sensing strategies for the active control of harmonic free field sound radiation.
8. S. E. WRIGHT and B. VUKSANOVIC 1999 *Journal of Sound and Vibration* **220**, 469–496. Active control of environmental noise, III. Implementation of theory into practice.
9. J. YANG and W. S. GAN 2000 *IEE Electronic Letters* **36**, 683–685. Speaker placement for robust virtual audio display system.
10. A. BASILEVSKY 1983 *Applied Matrix Algebra in the Statistical Sciences*. Amsterdam: Elsevier Science Publishing Co., Inc.
11. G. STRANG 1988 *Linear Algebra and its Applications*, 251. San Diego: Harcourt Brace Jovanovich; Chapter 5.

APPENDIX A

In the case of three-channel system, similar to the derivation of equation (4), the elements of 3×3 matrix $C^{\mathrm{H}}C$ are computed as follows:

$$C_1 = |C_{11}|^2 + |C_{51}|^2 + |C_{21}|^2, \tag{A1}$$

$$C_2 = C_{11}^* C_{15} + C_{51}^* C_{55} + C_{21}^* C_{25}, \tag{A2}$$

$$C_3 = 2|C_{11}C_{12}|\cos\phi + |C_{51}|^2, \tag{A3}$$

$$C_4 = |C_{55}|^2 + 2|C_{15}|^2. \tag{A4}$$

For the model shown in Figure 1, $C_{21} = C_{12}$, $C_{25} = C_{15}$, and the path difference $r_{15} - r_{11} \approx r_{12} - r_{15} = \delta r/2$, providing $c \gg (b + a)$. Then equation (A2) can be approximated as

$$C_2 \approx (1/r_{15})^2 2\cos(\phi/2) + (1/r_{55})^2 \mathrm{e}^{-\mathrm{j}k\eta}, \tag{A5}$$

where $\eta = r_{51} - r_{55}$ is a small quantity and its effect on the extreme value of $|C_2|$ can be ignored, compared to the first term on the right-hand side of equation (A5).

In the case of four-channel system, the elements of 4×4 matrix $C^{\mathrm{H}}C$ are computed as follows:

$$C_1 = |C_{11}|^2 + 2|C_{12}|^2 + |C_{13}|^2, \tag{A6}$$

$$C_2 = 2|C_{11}C_{12}|\cos\phi + 2|C_{12}C_{13}|\cos(\phi' - \phi), \tag{A7}$$

$$C_3 = 2|C_{11}C_{13}|\cos\phi' + 2|C_{12}|^2, \tag{A8}$$

where $\phi' = k\delta r' = k(r_{13} - r_{11})$, and it can be derived that $\delta r' \approx (\sqrt{2a})(\sqrt{2b})/2c = ab/c$. So $\phi' = 2\phi$ or $\delta r' = 2\delta r$, and equation (A7) can be simplified as

$$C_2 = 2(|C_{11}C_{12}| + |C_{12}C_{13}|)\cos\phi. \tag{A9}$$

In the case of six-channel system, the elements of 6×6 matrix $C^{\mathrm{H}}C$ are computed as follows:

$$C_1 = |C_{11}|^2 + |C_{51}|^2 + |C_{12}|^2 + |C_{13}|^2 + |C_{53}|^2 + |C_{14}|^2, \tag{A10}$$

$$C_2 = C_{11}^* C_{15} + C_{52}^* C_{55} + C_{12}^* C_{15} + C_{13}^* C_{16} + C_{53}^* C_{56} + C_{14}^* C_{16}, \tag{A11}$$

$$C_3 = |C_{51}|^2 + |C_{53}|^2 + 2(|C_{11}C_{12}| + |C_{12}C_{13}|)\cos\phi, \tag{A12}$$

$$C_4 = 2(|C_{11}C_{13}| + |C_{51}C_{53}|)\cos\phi' + 2|C_{12}|^2, \tag{A13}$$

$$C_5 = C_{11}^* C_{16} + C_{51}^* C_{56} + C_{12}^* C_{16} + C_{13}^* C_{15} + C_{53}^* C_{55} + C_{14}^* C_{15}, \tag{A14}$$

$$C_6 = 2(|C_{11}C_{12}| + |C_{12}C_{13}|)\cos\phi + 2|C_{51}C_{53}|\cos\phi', \tag{A15}$$

$$C_7 = 2|C_{15}|^2 + |C_{55}|^2 + 2|C_{16}|^2 + |C_{56}|^2, \tag{A16}$$

$$C_8 = 4(|C_{15}C_{16}| + 2|C_{55}C_{56}|)\cos\phi, \tag{A17}$$

where the phase difference is denoted as $k(r_{13} - r_{12}) \approx k(r_{16} - r_{15}) \approx k(r_{56} - r_{55}) \approx \phi$ and $k(r_{53} - r_{51}) \approx k(r_{13} - r_{11}) \approx \phi'$, providing $c \gg (b + a)$. Also, $C_{12} = C_{14}$ is used in the derivation. From equations (25) and (26),

$$A_1 A_2 = \begin{bmatrix} \alpha_1 & \alpha_2 & \alpha_3 \\ \alpha_4 & \alpha_5 & \alpha_4 \\ \alpha_3 & \alpha_2 & \alpha_1 \end{bmatrix}, \qquad A_2 A_1 = \begin{bmatrix} \alpha_1 & \alpha_4^* & \alpha_3 \\ \alpha_2^* & \alpha_5 & \alpha_2^* \\ \alpha_3 & \alpha_4^* & \alpha_1 \end{bmatrix}, \tag{A18, A19}$$

where

$$\alpha_1 = C_1C_4 + C_2C_5^* + C_3C_6, \qquad \alpha_2 = C_1C_5 + C_2C_8 + C_3C_5, \qquad \text{(A20, A21)}$$

$$\alpha_3 = C_1C_6 + C_2C_5^* + C_3C_4, \qquad \alpha_4 = C_2^*C_4 + C_5^*C_7 + C_2^*C_6, \qquad \text{(A22, A23)}$$

$$\alpha_5 = 2C_2^*C_5 + C_7C_8. \qquad \text{(A24)}$$

Clearly, $A_1A_2 \approx A_2A_1$ holds only if $\alpha_2 \approx \alpha_4^*$. Let $\gamma = (\alpha_2 - \alpha_4^*)/\alpha_2$, its real and imaginary parts, as a function of frequency, are drawn in Figure 4. It demonstrates that $\alpha_2 \approx \alpha_4^*$ resulting in $A_1A_2 \approx A_2A_1$, except at a few frequencies.